



A proton-coupled organic cation antiporter is involved in the blood-brain barrier transport of Aconitum alkaloids

Jiaojiao Cong^{a,b,1}, Yiling Ruan^{a,b,1}, Qinglin Lyu^b, Xiaohui Qin^{a,b}, Xinming Qi^c, Wenyuan Liu^{a,b}, Lifeng Kang^d, Junying Zhang^{b,**}, Chunyong Wu^{a,b,*}

^a Key Laboratory of Drug Quality Control and Pharmacovigilance, Ministry of Education, China Pharmaceutical University, No 24 Tongjia Road, Nanjing, 210009, China

^b China Pharmaceutical University, No 24 Tongjia Road, Nanjing, 210009, China

^c Shanghai Institute of Materia Medica, Chinese Academy of Sciences, No 501 Haik Road, Shanghai, 201203, China

^d School of Pharmacy, University of Sydney, Pharmacy and Bank Building A15, NSW 2006, Australia

ARTICLE INFO

Keywords:

Aconitum alkaloids
Blood-brain barrier
Proton-coupled organic cation antiporter
hCMEC/D3 cells
Drug transport

ABSTRACT

Ethnopharmacological relevance: The herbs of Aconitum are the essential Traditional Chinese medicine and have played an indispensable role in many Asian countries for thousands of years to treat critical illnesses, and chronic, stubborn diseases. However, Aconitum may induce severe neurotoxicity and even death. So far the mechanism of Aconitum penetrating the blood-brain barrier (BBB) is still unclear.

Aim of the study: To determine whether influx transporters contribute to the brain uptake of the highly toxic alkaloids in Aconitum including aconitine (AC), mesaconitine (MA) and hypaconitine (HA).

Materials and methods: The uptake of AC, MA and HA was characterized using *in vitro* hCMEC/D3 model and *in situ* mouse brain perfusion. In hCMEC/D3 cells, the effect of incubation temperature, time, initial drug concentration, energy (NaN₃), extracellular and intracellular pH (FCCP and NH₄Cl), the prototypical substrates/inhibitors of known organic cation transporting carriers and *trans*-stimulation (pre-incubating with pyrilamine and diphenhydramine) on the cellular uptake were studied. In addition, the effect of silencing OCTN1, OCTN2 and PMAT by specific siRNA was investigated. In mice, the contribution of the proton-coupled antiporter on the brain uptake of Aconitum was investigated by chemical inhibition.

Results: In hCMEC/D3 cells, AC, MA and HA were each taken up in a temperature-, time- and concentration-dependent manner, which were reduced by NaN₃ and FCCP. Regulation of extracellular and intracellular pH as well as *trans*-stimulation studies showed that AC, MA and HA were transported by a proton-coupled antiporter expressed at the plasma membrane that could also transport pyrilamine and diphenhydramine. Each uptake was markedly inhibited by various cationic drugs, but insensitive to the prototypical substrates/inhibitors of identified organic cation transporting carriers, such as OCTs, PMAT, MATs and OCTNs. In addition, silence of OCTN1, OCTN2 and PMAT had no significant inhibitory effect on the uptake of AC, MA and HA. In mice, the brain uptake of each alkaloid measured by *in situ* brain perfusion was suppressed by diphenhydramine when the transport capacity of P-gp/Bcrp at the BBB was chemically inhibited.

Conclusions: A novel proton-coupled organic cation antiporter plays a predominant role in the blood to brain influx of AC, MA and HA at the BBB, and thus affect the safety of Aconitum species.

1. Introduction

Since ancient time, Aconitum herbs have played an indispensable role in China and other Asian countries for the treatment of critical

illnesses, and chronic, stubborn diseases like collapse, syncope, cardiac dysfunction, rheumatism, painful joints, gastroenteritis, bronchial asthma and so on (Wu et al., 2018; Zhou et al., 2015; Nyirimigabo et al., 2015; Zhu et al., 2017). In Chinese Pharmacopoeia 2015, two Aconitum

* Corresponding author. China Pharmaceutical University, No.24 Tongjia Road, Nanjing, 210009, China.

** Corresponding author.

E-mail addresses: congjjiao@cpu.edu.cn (J. Cong), ryljessica@163.com (Y. Ruan), lyu@cpu.edu.cn (Q. Lyu), qxh_310@163.com (X. Qin), qxmng77777@gmail.com (X. Qi), liuwenyuan8506@163.com (W. Liu), lkang@alummi.nus.edu.sg (L. Kang), cpuzjy@cpu.edu.cn (J. Zhang), cywu@cpu.edu.cn (C. Wu).

¹ These two authors contributed equally to this article.

<https://doi.org/10.1016/j.jep.2020.112581>

Received 14 October 2019; Received in revised form 7 January 2020; Accepted 14 January 2020

Available online 20 January 2020

0378-8741/© 2020 Elsevier B.V. All rights reserved.

Abbreviations list

AC	Aconitine
HA	Hypaconitine
MA	Mesaconitine
BBB	Blood-brain barrier
BCRP	Breast cancer resistance protein
MATE	Multidrug and toxin extrusion transporters
MRP2	Multidrug resistance-associated protein 2

OCTs	Organic cation transporters
OCTNs	Organic cation/carnitine transporters
PMAT	Plasma membrane monoamine transporter
P-gp	P-glycoprotein
FCCP	Carbonyl cyanide 4-(trifluoromethoxy) phenylhydrazone
MPP ⁺	1-methyl-4-phenylpyridinium
TEA	Tetraethylammonium
qRT-PCR	Quantitative real-time PCR

species including the root of *Aconitum kusnezoffii* Reichb and *Aconitum camichaelii* Debx and approximate fifty herbal formulations containing Aconitum were recorded. Aconitum species have been proven to have anti-cancer, anti-inflammatory, anti-arrhythmia, and analgesic effects (Nyirimigabo et al., 2015; Liu et al., 2017; Ren et al., 2017; Zhang et al., 2017). Nonetheless, Aconitum has a narrow therapeutic index, and the improper preparation and usage might cause severe neurotoxicity, such as respiratory depression, unconsciousness and even death (Ameri, 1998; Singhuber et al., 2009; Li et al., 2016). To exert toxicological activities inside the brain, the toxic components of Aconitum need to cross the blood-brain barrier (BBB). Thus, a deep understanding of the factors contributing to the brain uptake will promote the safe and reasonable clinic application of Aconitum species.

The main highly toxic components of Aconitum species are diester-diterpenoid alkaloids, such as aconitine (AC), mesaconitine (MA) and hypaconitine (HA) (Liu et al., 2017; Singhuber et al., 2009). AC, MA and HA may be the substrates of ATP-binding cassette efflux transporters including P-glycoprotein (P-gp) (Zhu et al., 2017; Yang et al., 2013; Ye et al., 2013), breast cancer resistance protein (BCRP) (Ye et al., 2013), and multidrug resistance-associated protein 2 (MRP2) (Ye et al., 2013; Dai et al., 2015). Hence, we hypothesized that the BBB is also equipped with some active influx transporters, which can mediate the brain penetration of AC, MA and HA, and thus counteracting these efflux transporters to cause the neurotoxicity.

As AC, MA and HA have tertiary amine moieties and are positively charged at physiological pH, they may be the substrates of organic cation transporting carriers, such as organic cation transporters (OCTs), plasma membrane monoamine transporter (PMAT), multidrug and toxin extrusion transporters (MATEs), and organic cation/carnitine transporters (OCTNs) that have been identified at the gene level (Wu et al., 2016). Recently, a novel pyrrolamine-sensitive proton/organic cation antiporter was identified at the function level on the intestine, BBB and liver, and was proven to mediate the influx of various cationic drugs, such as nicotine (Tega et al., 2015), pyrrolamine (Okura et al., 2008; Shimomura et al., 2013), matrine (Wu et al., 2016), tramadol (Kitamura et al., 2014), clonidine (André et al., 2009) and diphenhydramine (Mizuuchi et al., 2000; Sadiq et al., 2011). Although the molecular nature of this antiporter is still unknown, it is distinct from any of the well-known organic cation transporting carriers.

The objective of this study is therefore to elucidate the influx mechanism of AC, MA and HA across the BBB using the immortalized human brain capillary endothelial cells (hCMEC/D3) and *in situ* mouse brain perfusion models.

2. Materials and methods

2.1. Chemicals

Aconitine (AC, purity > 98%), mesaconitine (MA, purity > 98%) and hypaconitine (HA, purity > 98%) were purchased from Biopurify Phytochemicals Ltd. (China). Olaparib was purchased from Pharmacodia Co., Ltd. (China). Methanol of HPLC grade was purchased from Merck KGaA (Germany). HEPES, penicillin-streptomycin, and sodium pyruvate were purchased from Gibco (USA). All other solvents

and chemicals were analytical grade and commercially available.

2.2. Animals

Male ICR mice weighing approximately 20 g were purchased from Qinglong Mountain Animal Breeding Farm (Nanjing, China), and were used following the protocols approved by the Animal Care Committee of China Pharmaceutical University. The mice were housed under controlled standard conditions with 12/12 h light/dark cycles and were fasted but allowed water *ad libitum* for 12 h prior to AC, MA and HA administration.

2.3. Uptake studies in hCMEC/D3 cells

The hCMEC/D3 cell line was purchased from Merck Pte Ltd. (Singapore) and was cultured in EBM-2 medium (Lonza, USA) supplemented with EGM-2 MV BulletKits (Lonza, USA) containing fetal bovine serum (5%), hydrocortisone, propeptide R3 insulin-like growth factor (R3-IGF), vascular endothelial growth factor (VEGF), basic human fibroblast growth factor (hFGF-B), ascorbic acid, human endothelial growth factor (hEGF) and gentamicin sulfate-amphotericin. Cells were cultured at 37 °C under 5% CO₂ and 95% humidity.

The uptake experiment was performed as described previously (Poller et al., 2008; Takahashi et al., 2018), with some modifications. In brief, hCMEC/D3 cells were seeded at a density of 1×10^5 cells/well on collagen I-coated 12-well plates (Corning, USA). The cells grown to 80%–90% confluence were washed and pre-incubated with HBSS-P buffer (138 mM NaCl, 5.33 mM KCl, 0.441 mM KH₂PO₄, 0.338 mM Na₂HPO₄, 0.407 mM MgSO₄, 0.493 mM MgCl₂, 10 mM HEPES, 5.56 mM glucose, 1.26 mM CaCl₂, 4.17 mM NaHCO₃ and 1 mM Na-Pyruvate, pH 7.4 unless otherwise specified) for 30 min at 37 °C. The uptake was initiated by adding 0.8 ml of the buffer containing AC, MA and HA (each at 0.5 μM unless otherwise specified). After incubation at 37 °C for 1 min unless otherwise specified, the cells were washed three times with 1 ml of the ice-cold buffer to end the uptake. The cells were collected in 300 μl of water, followed by homogenization with ultrasonic treatment. The homogenates were preserved at −80 °C until analysis. BCA protein assay kit (Thermo Fisher Scientific, USA) was used to analyze the cellular protein amount. The uptake of AC, MA and HA expressed as the cell-to-medium ratio (μl/mg protein) was calculated by equation (1).

$$\text{Cell-to-medium ratio} = A \times 1000 / S \quad (1)$$

where *A* is the cellular uptake amount (nmol/mg protein), *S* is the corresponding concentration of the incubation buffer (μM).

In the concentration-dependent study, the initial uptake of AC, MA and HA (0.5–800 μM, for 1 min) were fitted to equation (2) using nonlinear least-squares regression analysis (Graphpad Prism, USA).

$$V = V_{\max} \times S / (K_m + S) + P_{\text{diff}} \times S \quad (2)$$

where *V* and *V*_{max} are the initial uptake rate and the maximum uptake rate (nmol/min/mg protein), respectively. *K*_m is the Michaelis-Menten constant (μM). *S* is the concentration of AC, MA and HA in the incubation buffer (μM). *P*_{diff} is the passive diffusion clearance (ml/min/mg

protein).

The uptake was further performed in the presence of 0.1% sodium azide (NaN_3) or 25 μM carbonyl cyanide 4-(trifluoromethoxy) phenylhydrazone (FCCP) to investigate the effect of energy or proton gradient on the drug accumulation in hCMEC/D3 cells. To investigate the effect of extracellular pH (pH_e), the uptakes at pH 6.4 and 8.4 were compared with that at pH 7.4. To investigate the effects of intracellular pH (pH_i), the presence of 30 mM NH_4Cl during drug incubation (Acute) or pre-incubation (Pre) was used to create alkaline or acidic pH_i (Wu et al., 2016). To identify the potential drug transporter, the effects of specific inhibitors of identified organic cation transporting carriers were studied on the uptake of AC, MA and HA (each at 0.5 μM for 1 min). In the *trans*-stimulation experiment, cells pre-incubated with pyrilamine or diphenhydramine (each at 0.5 mM) for 30 min were washed with pre-warmed buffer and incubated with the buffer containing AC, MA and HA (each at 0.5 μM) for 1 min.

2.4. RNA interference analysis

For gene silencing, different sets of siRNAs specific for OCTN1 (OCTN1 siRNA), OCTN2 (a mixture of OCTN2 siRNA1, siRNA2 and siRNA3), PMAT (PMAT siRNA) and negative control (NC siRNA) (Table 1) were purchased from Genescript (China). The RNA interference analysis was carried out as described before (Takahashi et al., 2018), with slight modifications. In brief, hCMEC/D3 cells seeded on collagen I-coated 12-well plates (Corning, USA) at the density of 4×10^4 cells/well were transfected with siRNA at different final concentrations (10–100 nM for RNA extraction, 10 nM for cellular uptake) by using Lipofectamine RNAiMAX (1.6 μl /well, Invitrogen). 72 h after transfection, quantitative real-time PCR (qRT-PCR) and cellular uptake studies were performed.

2.5. Total RNA isolation and qRT-PCR

The expression of organic cation transporting carriers (OCTN1, OCTN2, PMAT) and the housekeeping gene (GAPDH) in hCMEC/D3 cells at mRNA levels were determined by qRT-PCR. Trizol (Invitrogen, USA) was used to isolate the total RNA, which was used as templates to prepare the single-strand cDNA by using PrimeScript RT Master Mix (Takara, Japan). The qRT-PCR analysis was performed using QIAGEN Rotor-Gene Q (Germany) with SYBR Premix Ex Taq II (RR420A) (Takara, Japan) following the manufacturer's protocols. The primer sets listed in Table 2 were purchased from Sangon Biotech Co. Ltd (China). The thermal protocol was set to 2 min at 50 °C, followed by 30 s at 95 °C, 40 cycles of 5 s at 95 °C and then 40 s at 60 °C.

2.6. In situ mouse brain perfusion study

The perfusion model was established as previously described (Gynther et al., 2016), with some modifications. In short, mice anesthetized with pentobarbital (52 mg/kg, i.p.) were placed on a hot plate (37 °C). The right common carotid artery was ligated and catheterized with a polyethylene tubing (0.5 mm o.d.). Immediately after severing the heart, the perfusion was started at a flow rate of 2 ml/min

Table 2
Primers for qRT-PCR.

Target	Sense	Antisense
OCTN1	TGGTAGCCTTCATACTAGGAACA	TGGCAGCAGCATATAGCCAAC
OCTN2	TCCACCATTTGTGACCGAGTG	ACCCACGAAGAACAAGGAGATT
PMAT	GCTTTCACGGATACTACATTGGA	ATGTCAAACACGATGGAGGTC
GAPDH	GGTGGTCTCTCTGACTTCAACA	GTTGCTGTAGCCAATTCGTTGT

using an infusion pump (Harvard Apparatus, USA). The perfusion fluid was Krebs–Henseleit buffer (25 mM NaHCO_3 , 4.7 mM KCl, 118 mM NaCl, 1.2 mM $\text{MgSO}_4 \cdot 7\text{H}_2\text{O}$, 1.2 mM $\text{CaCl}_2 \cdot 2\text{H}_2\text{O}$, 1.2 mM $\text{NaH}_2\text{PO}_4 \cdot 2\text{H}_2\text{O}$ and 10 mM D-glucose), warmed to 37 °C and gassed with 95% O_2 /5% CO_2 (pH 7.4). Each mouse was perfused with AC, MA and HA at 5 μM in the absence or presence of the tested inhibitors. After 1 min perfusion, the right cerebral hemisphere was anatomized and accurately weighed. An aliquot of the perfusion fluid was collected from the end of the tubing. The brain and perfusion fluid samples were stored at –80 °C until analysis.

The initial uptake clearance (Cl_{up} , ml/g/min) of the test drug was obtained by equation (3).

$$Cl_{up} = X_{\text{brain}} / (T \times C_{\text{perf}}) \quad (3)$$

where X_{brain} is the amount of the test drug in brain (nmol/g), T is the perfusion time (min), and C_{perf} is the drug concentration in the perfusion fluid (μM).

2.7. HPLC-MS/MS analysis

Brain tissues were homogenized with 3-fold normal saline. 140 μl of the cell homogenates or 100 μl of the brain homogenates were added with 20 μl of olaparib solution (0.5 $\mu\text{g}/\text{ml}$) as the internal standard (IS), and 40 μl of methanol for the cell sample or 280 μl of acetonitrile for the brain sample. The mixture was vortexed for 3 min. After centrifugation at 12000 rpm for 5 min, 20 μl of the supernatant was injected into LC-30AD liquid chromatography (Shimadzu, Japan) coupled with an AB SCIEX Triple Quad™ 5500 (SCIEX, USA).

The separation was achieved on a Heder ODS-2 C18 column (4.6 mm \times 150 mm, 5 μm) at 30 °C. 10 mM ammonium acetate solution containing 0.1% formic acid - methanol (30:70, v/v) was used as the mobile phase, which was delivered at 0.8 ml/min. The eluate was split and loaded into the MS via the ESI source. The analytes were detected using multiple reaction monitoring (MRM) in the positive mode. The transition was m/z 646.3 \rightarrow 586.2 for AC, 632.2 \rightarrow 572.2 for MA, 616.3 \rightarrow 556.2 for HA and 435.2 \rightarrow 367.2 for IS. The ionspray voltage and temperature were 4 kV and 500 °C. The curtain gas pressure, GS1 pressure and GS2 pressure was 40, 40 and 50 psi. The collision energy of dissociation was set at 46, 42, 41 and 28 eV for AC, MA, HA and IS, respectively.

2.8. Statistical analysis

Data were presented as mean \pm standard deviation (SD). Statistical analysis was carried out using unpaired Student's *t*-test for single

Table 1
siRNA sequences used in the transfection experiments.

Gene name	siRNA name	Sense	Antisense
OCTN1	OCTN1siRNA	CCAACU AUGUGGUAGCCUUTT	AAGGCUACCAUAGUUGGTT
OCTN2	OCTN2 siRNA1	GCAGCUGUCAGACAGGUUUTT	AAACUGUCUGACAGCUGCTT
	OCTN2 siRNA2	GCAGCAGUCCCAACAUAUUTT	AAUGUUGUGGACUGCUGCTT
	OCTN2 siRNA3	GCAUCCUGUCUCCUACUUTT	AAGUAGGAGACAGGAUGCTT
PMAT	PMAT siRNA	CCAUGACCGUGUCCUACAUTT	AUGUAGGACAGGUGAUGGTT
NC	NC siRNA	UUCUCGGAACGUGUCAGGUTT	ACGUGACACGUCGAGAATT

Abbreviation: NC = negative control.

comparison and one-way ANOVA with Dunnett's test for multiple comparisons. $P < 0.05$ was considered statistically significant.

3. Results and discussion

3.1. Effect of time and temperature on cellular uptake

hCMEC/D3 cell line is a well-established *in-vitro* BBB model (Takahashi et al., 2018), which is known to express ATP-binding cassette (ABC) transporters and solute carrier (SLC) transporters (Ohtsuki et al., 2013; Okura et al., 2014; Weksler et al., 2013). Moreover, a novel pyrilamine-sensitive proton-coupled organic cation antiporter also functions in this cell line (Shimomura et al., 2013; Kitamura et al., 2014; Higuchi et al., 2015). As shown in Fig. 1, AC, MA and HA were taken up into hCMEC/D3 cells in a time- and temperature-dependent manner. After 1 min incubation, the uptake of AC, MA and HA at 4 °C was 4.8%, 6.1% and 3.8% of that at 37 °C, indicating that a carrier protein may participate in the accumulation of AC, MA and HA in hCMEC/D3 cells. The initial uptake at 1 min was selected for the subsequent studies.

3.2. Effect of drug concentration on cellular uptake

As shown in Fig. 2, the initial uptake of AC, MA and HA was also concentration-dependent (Fig. 2). Eadie-Hofstee plot for each uptake showed one straight line indicating a single saturable process for each alkaloid. The values of K_m and V_{max} calculated by the kinetic analysis are shown in Table 3. At the concentration of 0.5 μM , the saturable uptake of AC, MA and HA calculated by the kinetic parameters attributed 94.3%, 84.2% and 97.9% of the total cellular influx, respectively. These results indicated that a saturable active carrier-mediated transport process played a major role in the uptake of AC, MA and HA.

3.3. Effect of metabolic energy on cellular uptake

ATP-depleted hCMEC/D3 cells were established by treating cells with 0.1% NaN_3 , a metabolic inhibitor. As illustrated in Fig. 3, the uptake of AC, MA and HA was significantly decreased in ATP-depleted cells, indicating that the uptake of each alkaloid relies on the metabolic energy.

3.4. Effect of pH on cellular uptake

Next, the effects of pH on the cellular uptake were investigated. The uptake of AC, MA and HA in hCMEC/D3 cells was decreased in the presence of 25 μM FCCP, which is a protonophore (Fig. 4) indicating that each transport is driven by the proton electrochemical difference.

Then the uptake of each alkaloid was evaluated under different extracellular and intracellular pH values. As shown in Fig. 5A, the uptake of AC, MA and HA was lowered at pH_e 6.4 but elevated at pH_e 8.4. To elucidate whether such an effect is due to the changing ratio of the neutral form of each analyte or the modulation of the uptake rate according to the proton gradient, the effects of intracellular pH regulated by NH_4Cl (Wu et al., 2016) on the cellular accumulation were further examined. As shown in Fig. 5B, acute treatment with NH_4Cl (intracellular alkalinization) markedly inhibited the uptake of AC, MA and HA into hCMEC/D3 cells. On the contrary, NH_4Cl pretreatment (intracellular acidification) significantly stimulated the uptake of each alkaloid. All these results suggested that the involved influx transporter for AC, MA and HA was driven by an oppositely directed proton gradient. As the intracellular pH in rat brain capillary endothelial cells was 6.9–7.15 (Okura et al., 2008), lower intracellular pH can drive the influx of Aconitum alkaloids into brain.

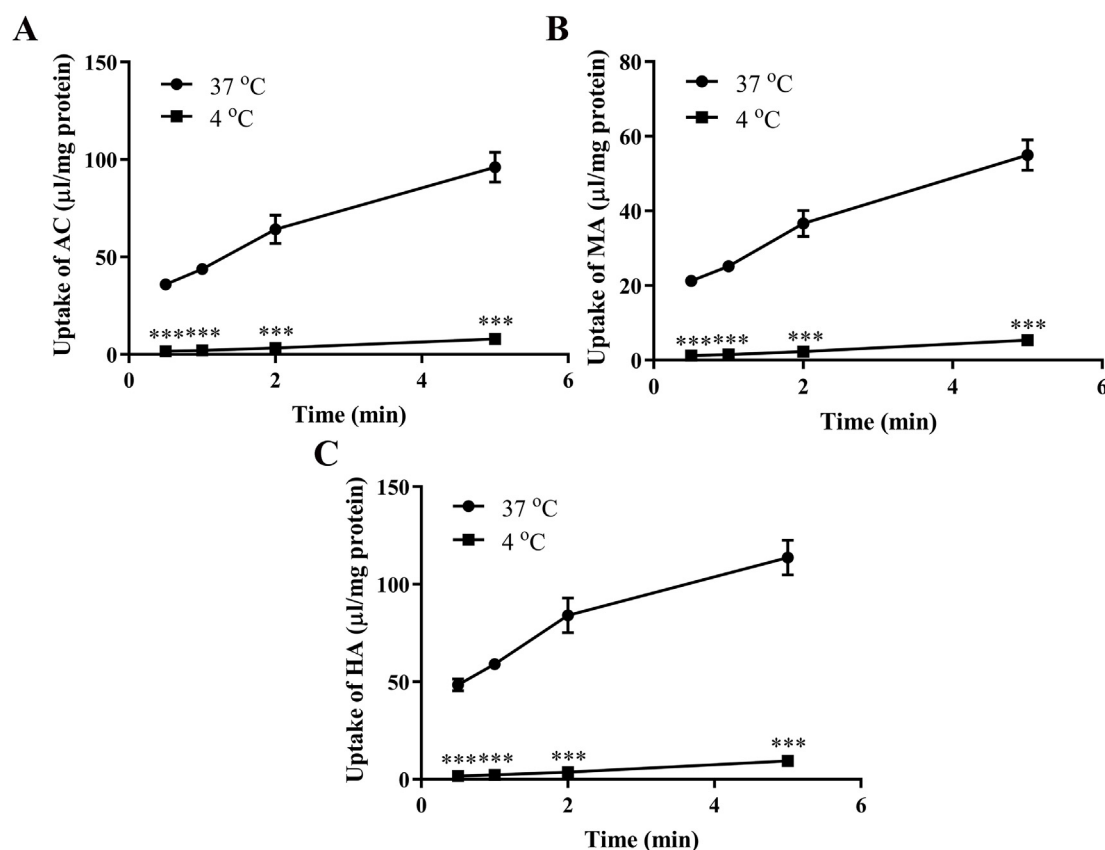


Fig. 1. Time and temperature dependence of (A) aconitine (AC), (B) mesaconitine (MA) and (C) hypaconitine (HA) uptake by hCMEC/D3 cells. The uptake of AC, MA and HA (each at 0.5 μM) was measured at 37 °C (●) and 4 °C (■). Each point represents the mean \pm SD of three determinations. ***, $P < 0.001$ versus 37 °C.

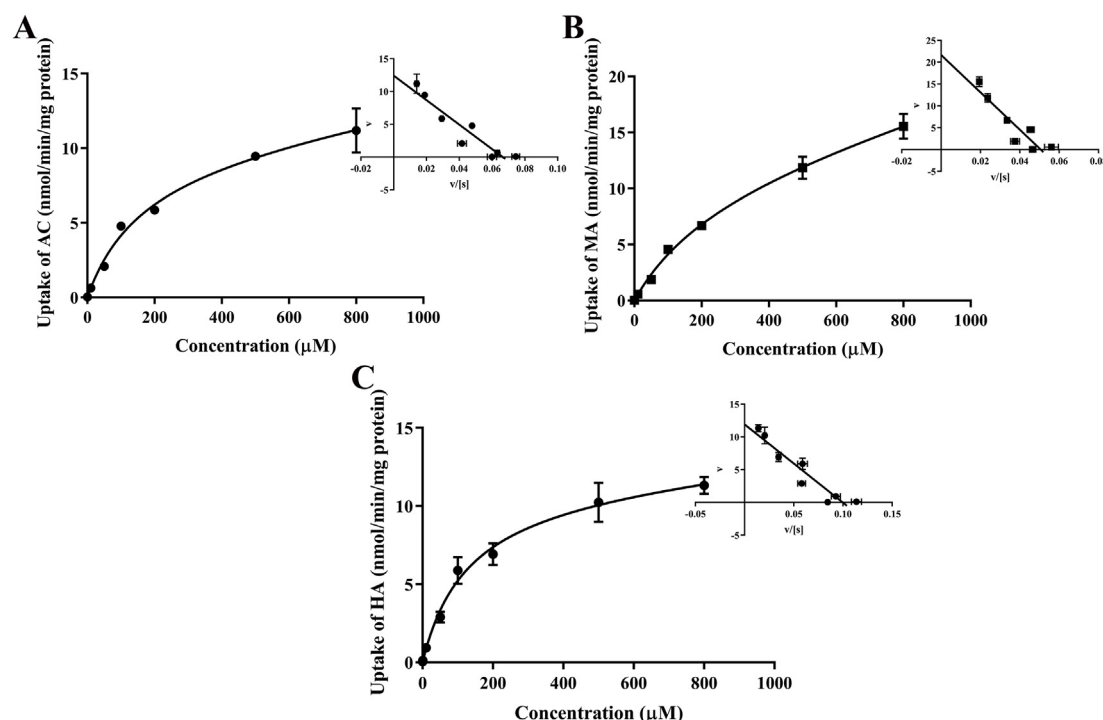


Fig. 2. Concentration dependence of (A) aconitine (AC), (B) mesaconitine (MA) and (C) hypaconitine (HA) uptake by hCMEC/D3 cells. Uptake of AC, MA and HA at 0.5–800 μM was measured at 37 $^{\circ}\text{C}$ for 1 min. The inset shows the Eadie-Hofstee plot of each uptake. V and S represent the initial uptake velocity (nmol/min/mg protein) and concentration (μM). Each point represents the mean \pm SD of three determinations.

Table 3

Kinetic analysis of the cellular uptake.

Parameters	AC	MA	HA
V_{\max} (nmol/min/mg protein)	9.94	11.4	11.4
K_m (μM)	163	249	126
P_{diff} ($\mu\text{l}/\text{min}/\text{mg}$ protein)	3.70	8.54	1.95

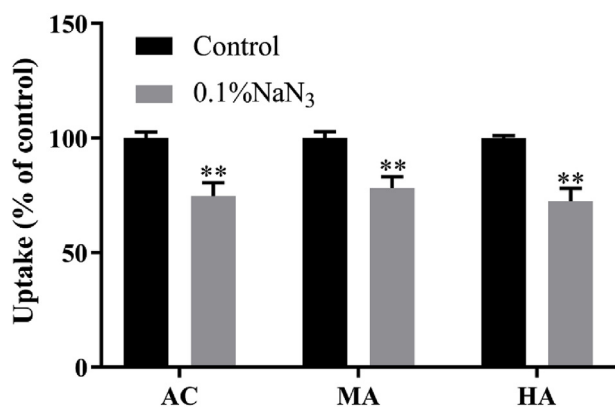


Fig. 3. Effect of ATP depletion on aconitine (AC), mesaconitine (MA) and hypaconitine (HA) uptake by hCMEC/D3 cells. The uptake of AC, MA and HA (each at 0.5 μM) was measured at 37 $^{\circ}\text{C}$ for 1 min in the absence and presence of 0.1% NaN_3 . Each column represents the mean \pm SD of three determinations. **, $P < 0.01$ versus control.

3.5. Inhibition study on cellular uptake

To identify the influx transporter responsible for the uptake of AC, MA and HA, the *cis*-inhibition study was performed (Table 4). The uptake was significantly inhibited by the organic cation compounds, such as pyrilamine, verapamil, quinidine, diphenhydramine and

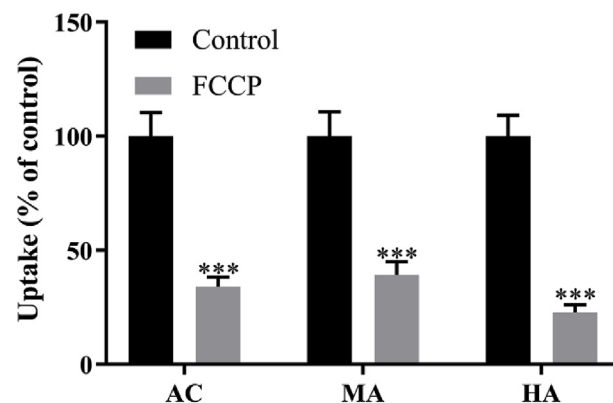


Fig. 4. Effect of protonophore on aconitine (AC), mesaconitine (MA) and hypaconitine (HA) uptake by hCMEC/D3 cells. Uptake of AC, MA and HA each at 0.5 μM was measured at 37 $^{\circ}\text{C}$ for 1 min in the absence and presence of 25 μM FCCP. Each column represents the mean \pm SD of three determinations. ***, $P < 0.001$ versus control.

amantadine, indicating the involvement of organic cation transporting carriers. However, the influx process of each alkaloid was not sensitive to tetraethylammonium (TEA) and 1-methyl-4-phenylpyridinium (MPP^+) (substrates of OCTs, OCTNs, MATEs and PMAT) (Ahmadimoghaddam et al., 2012; Damme et al., 2011; Engel and Wang, 2005; Zhou et al., 2017), pyrimethamine (specific inhibitor of MATEs) (Ito et al., 2010), L-carnitine (substrate of OCTN2) (Okura et al., 2014) and ergothioneine (substrate of OCTN1) (Li et al., 2014). Hence, AC, MA and HA are likely transported by a novel organic cation transporting carrier rather than the identified OCTs, PMAT, MATEs and OCTNs. Such inhibition features are very similar to that of a recently discovered pyrilamine-sensitive proton-coupled organic cation antiporter (Wu et al., 2016; Tega et al., 2015; Shimomura et al., 2013; Mizuuchi et al., 2000; Higuchi et al., 2015; Wang et al., 2017).

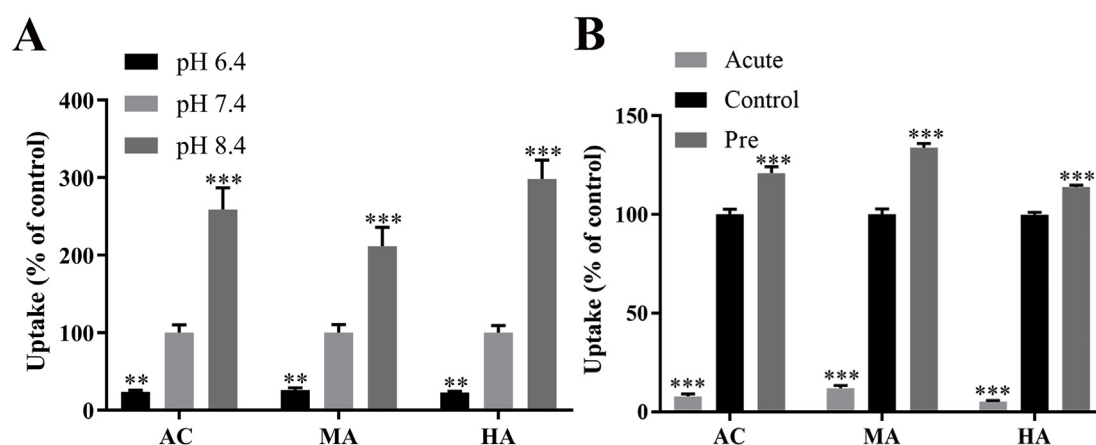


Fig. 5. Effects of (A) extracellular pH and (B) intracellular pH on aconitine (AC), mesaconitine (MA) and hyaпонitine (HA) uptake by hCMEC/D3 cells. (A) The uptake of AC, MA and HA (each at 0.5 μ M) was measured at buffer pH of 6.4, 7.4 and 8.4. (B) The cells were pre-incubated in the absence (Control and Acute) or presence (Pre) of 30 mM NH_4Cl for 30 min, followed by incubation with AC, MA and HA for 1 min in the absence (Control and Pre) or presence (Acute) of 30 mM NH_4Cl . Each column represents the mean \pm SD of three determinations. **, $P < 0.01$; ***, $P < 0.001$ versus pH 7.4 or control.

3.6. RNA interference analysis

To further confirm the above findings in the *cis*-inhibition study, knockdown experiments using siRNA were performed. It has been reported that OCTNs and PMAT are abundantly expressed while the expression of OCTs and MATes are negligible in hCMEC/D3 cells (Shimomura et al., 2013). Thus, the effects of OCTN1, OCTN2 and PMAT knockdown using specific siRNA (Table 2) on the uptake of each alkaloid were investigated. siRNA of each target gene was investigated at different concentrations, and 10 nM was enough to silence OCTN1, OCTN2 and PMAT in hCMEC/D3 cells (Fig. 6). As expected, specific siRNA targeting OCTN1, OCTN2 and PMAT had no significant inhibitory effect on the uptake of AC, MA and HA (Fig. 7), thus excluding the major contribution of these well-known organic cation transporting carriers.

3.7. Trans-stimulation study on cellular uptake

To exclude the possibility that the uptake of AC, MA and HA is attributable to the binding to the cell membrane surface or intracellular components, and to recognize the relevant transporter, the *trans*-stimulation study was carried out. The uptake of AC, MA and HA was markedly increased by pre-treating hCMEC/D3 cells for 30 min with pyrilamine or diphenhydramine (Fig. 8), indicating that the uptake of each Aconitum alkaloid into hCMEC/D3 cells is due to an antiporter expressed at the plasma membrane that could transport pyrilamine and

diphenhydramine, further confirming that the involved antiporter is the pyrilamine-sensitive proton-coupled organic cation antiporter.

3.8. In situ mouse brain perfusion study

The BBB transport properties of Aconitum alkaloids were finally characterized using the *in situ* mouse brain perfusion method, in which an artificial perfusate fluid replaced the blood. Since the transporter is exposed to the drug directly at selected unbound concentrations, this method could accurately investigate the BBB permeability (André et al., 2009; Chapy et al., 2016). Firstly, the inhibitors of ABC transporters were used to investigate the role of efflux transporters involved in handling AC, MA and HA (Fig. 9). At mouse BBB, GF120918 (inhibitor of P-gp/Bcrp) but not probenecid (inhibitor of Mrp2) led to a significant increase in the brain uptake of AC, MA and HA, suggesting that P-gp/Bcrp, rather than Mrp2, limited the brain distribution of AC, MA and HA.

Then the effect of diphenhydramine, an inhibitor of the pyrilamine-sensitive proton-coupled organic cation antiporter, on the brain transport of AC, MA and HA was investigated (Fig. 10). When P-gp/Bcrp activity was chemically inhibited by GF120918, diphenhydramine significantly suppressed the brain uptake of AC, MA and HA, unveiling the indispensable role of the influx transporter on the brain initial uptake of AC, MA and HA.

Table 4
Inhibitory effects of selected compounds on AC, MA and HA uptake by hCMEC/D3 cells.

Compound	Concentration (mmol/l)	Uptake of AC	Uptake of MA	Uptake of HA
		(% of control)	(% of control)	(% of control)
Control		100.0 \pm 2.6	100.0 \pm 2.8	100.0 \pm 1.0
Pyrilamine	1	41.4 \pm 2.1***	46.1 \pm 1.4***	30.6 \pm 1.5***
Quinidine	1	11.4 \pm 2.0***	19.6 \pm 3.7***	6.6 \pm 1.4***
Verapamil	0.5	19.6 \pm 2.2***	27.8 \pm 2.8***	11.6 \pm 1.0***
Diphenhydramine	1	24.2 \pm 0.3***	32.2 \pm 0.9***	17.4 \pm 0.3***
Amantadine	1	56.3 \pm 5.4***	62.2 \pm 6.0***	44.2 \pm 4.6***
TEA	1	87.8 \pm 2.7*	92.1 \pm 4.5	85.9 \pm 3.5*
MPP ⁺	1	93.8 \pm 7.1	107.1 \pm 6.6	92.4 \pm 8.0
Pyrimethamine	0.1	91.2 \pm 3.9	106.5 \pm 1.5	89.6 \pm 9.0
L-carnitine	1	96.2 \pm 2.8	107.3 \pm 2.8	99.5 \pm 2.3
Ergothioneine	0.5	111.9 \pm 9.6*	111.1 \pm 4.2*	110.1 \pm 10.6

The uptake of AC, MA and HA (each at 0.5 μ M) was measured at 37 $^{\circ}\text{C}$ for 1 min in the absence (Control) and presence of each selected compound. Each value represents mean \pm SD of three determinations. *, $P < 0.05$; **, $P < 0.01$; ***, $P < 0.001$ versus control.

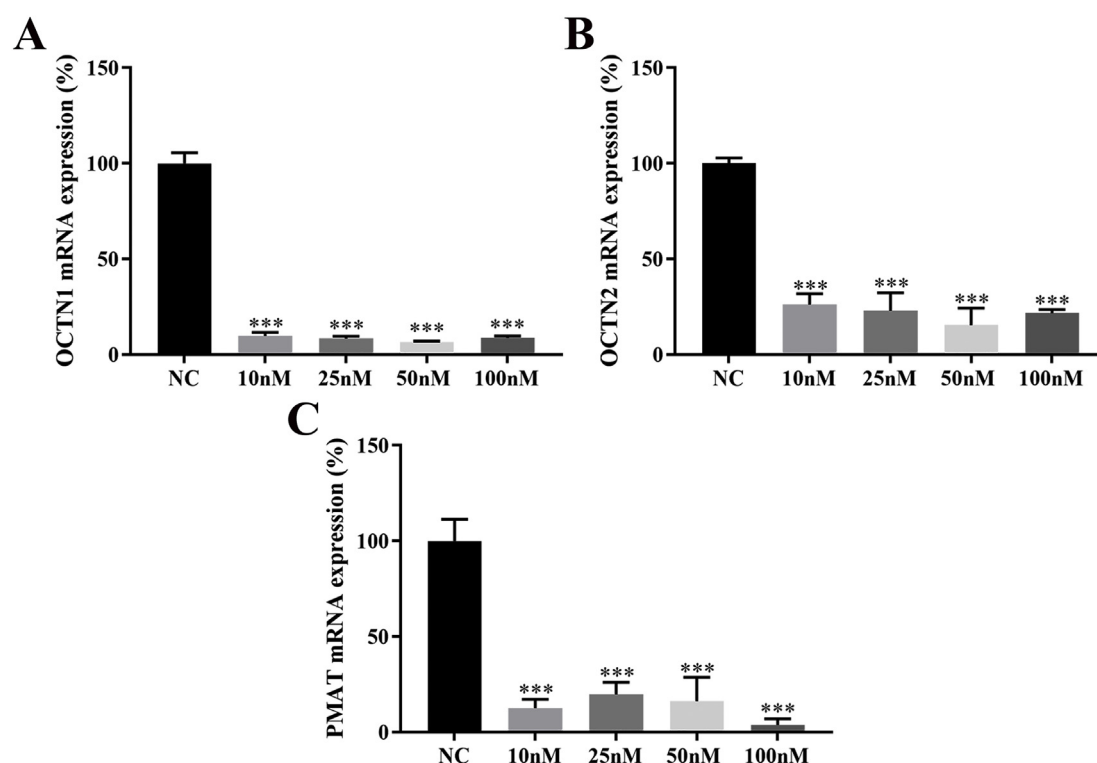


Fig. 6. Gene silencing effects of (A) OCTN1, (B) OCTN2 and (C) PMAT siRNA after 72h transfection in hCMEC/D3 cells. Each column represents the mean \pm SD of three determinations. ***, $P < 0.001$ versus negative control (NC) group.

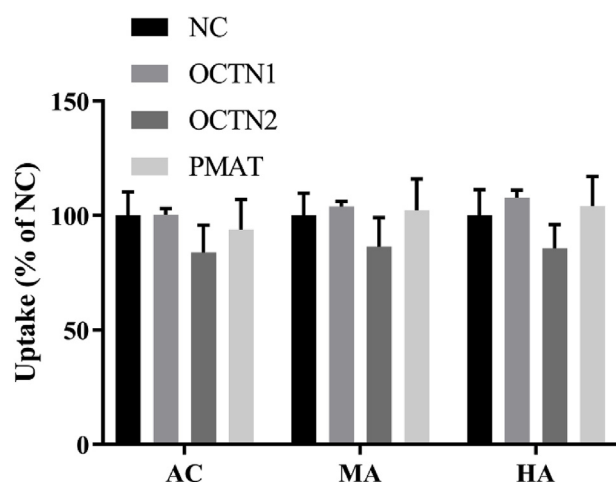


Fig. 7. Effects of OCTN1, OCTN2 and PMAT silence on AC, MA and HA uptake by hCMEC/D3 cells. 72 h after the cells were transfected with negative control (NC), OCTN1, OCTN2 or PMAT siRNA, the uptake of aconitine (AC), mesaconitine (MA) and hyaonitine (HA) (each at 0.5 μ M) was measured at 37 $^{\circ}$ C for 1 min. Each column represents the mean \pm SD of three determinations. No statistical differences were observed.

4. Conclusion

This study elucidates the brain transport mechanism of the neurotoxic Aconitum alkaloids across the BBB. Characterization of the uptake properties in hCMEC/D3 cells and *in situ* mouse brain perfusion models demonstrate that the pyrilamine-sensitive proton-coupled organic cation antiporter plays an important role in the brain uptake of AC, MA and HA, and might have a significant impact on the safety of Aconitum species. Further studies are necessary to determine whether commonly used cationic drugs or herbs containing cationic components may cause transporter-mediated drug-drug interactions in clinical practice.

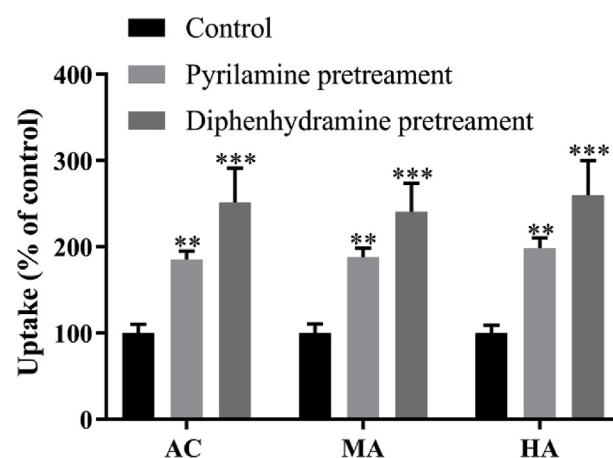


Fig. 8. Trans-stimulation effects on aconitine (AC), mesaconitine (MA) and hyaonitine (HA) uptake by hCMEC/D3 cells. After pre-incubation for 30 min in the absence (Control) and presence of pyrilamine (0.5 mM) or diphenhydramine (0.5 mM), the cells were washed and then incubated with AC, MA and HA (each at 0.5 μ M) for 1 min at 37 $^{\circ}$ C. Each column represents the mean \pm SD of three determinations. **, $P < 0.01$; ***, $P < 0.001$ versus control.

Author contribution statement

C.W. conceived and J.C. designed the study. J.C., Y.R. and XH.Q. carried out the experiments and all authors discussed the results. J.C. wrote the manuscript and Q.L. XM.Q. W.L. L.K. and J.Z. provided critical feedback. C.W. and Y.R. revised the manuscript and submitted for publication.

Declaration of competing interest

The authors report no conflicts of interest. The authors alone are responsible for the content and writing of this article.

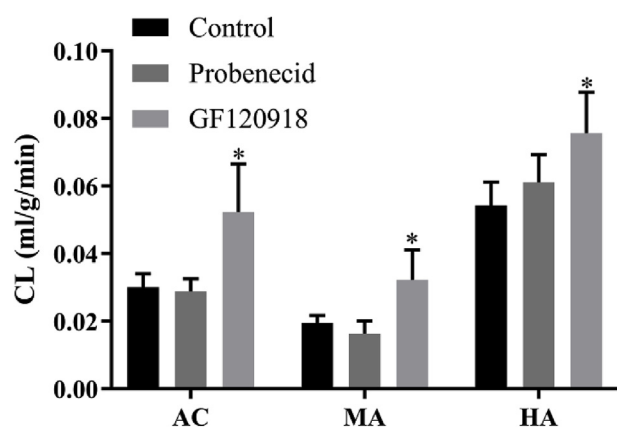


Fig. 9. Effects of the inhibitors of P-gp, Bcrp and Mrp2 on the brain uptake of aconitine (AC), mesaconitine (MA) and hyaconitine (HA). Perfusate containing AC, MA and HA (each at 5 μ M) with or without GF120918 (20 μ M) or probenecid (1 mM) was perfused into the brain hemisphere at 2 ml/min for 1 min. Each column represents the mean \pm SD of four mice. *, $P < 0.05$ versus control group.

Abbreviation: CL = the initial uptake clearance.

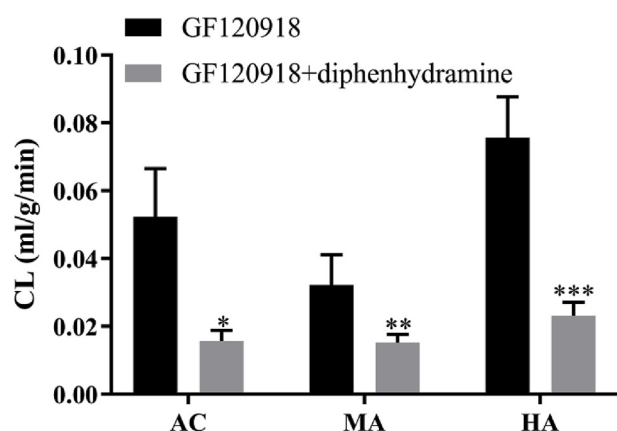


Fig. 10. Effect of diphenhydramine on the brain uptake of aconitine (AC), mesaconitine (MA) and hyaconitine (HA) in mice. The transport of AC, MA and HA (each at 5 μ M) was measured in mice perfused with GF120918 (20 μ M) alone (control) or GF120918 (20 μ M) plus diphenhydramine (30 mM). Each column represents the mean \pm SD of four mice. *, $P < 0.05$; **, $P < 0.01$; ***, $P < 0.001$ versus GF120918 group.

Abbreviation: CL = the initial uptake clearance.

Acknowledgements

This work was supported by the National Natural Science Foundation of China (Nos. 81673681, 81473357), the "Double First-Class" University project (No. CPU2018GY34) and the Priority Academic Program Development of Jiangsu Higher Education Institutions.

References

- Ahmadimoghaddam, D., Hofman, J., Zemankova, L., Nachtigal, P., Dolezelova, E., Cerveny, L., Ceckova, M., Micuda, S., Staud, F., 2012. Synchronized activity of organic cation transporter 3 (Oct3/Slc22a3) and multidrug and toxin extrusion 1 (MATE1/Slc47a1) transporter in transplacental passage of MPP+ in rat. *Toxicol. Sci.* 128, 471–481. <https://doi.org/10.1093/toxsci/kfs160>.
- Ameri, A., 1998. The effects of Aconitum alkaloids on the central nervous system. *Prog. Neurobiol.* 56, 211–235. [https://doi.org/10.1016/S0304-0082\(98\)00037-9](https://doi.org/10.1016/S0304-0082(98)00037-9).
- André, P., Debray, M., Scherrmann, J.-M., Cisternino, S., 2009. Clonidine transport at the mouse blood-brain barrier by a new H⁺ antiporter that interacts with addictive drugs. *J. Cereb. Blood Flow Metab.* 29, 1293–1304. <https://doi.org/10.1038/jcbfm.2009.54>.
- Chapy, H., Saubaméa, B., Tournier, N., Bourasset, F., Behar-Cohen, F., Declèves, X.,

- Scherrmann, J.-M., Cisternino, S., 2016. Blood-brain and retinal barriers show dissimilar ABC transporter impacts and concealed effect of P-glycoprotein on a novel verapamil influx carrier. *Br. J. Pharmacol.* 173, 497–510. <https://doi.org/10.1111/bph.13376>.
- Dai, P., Zhu, L., Yang, X., Zhao, M., Shi, J., Wang, Y., Lu, L., Liu, Z., 2015. Multidrug resistance-associated protein 2 is involved in the efflux of Aconitum alkaloids determined by MRP2-MDCKII cells. *Life Sci.* 127, 66–72. <https://doi.org/10.1016/j.lfs.2015.02.011>.
- Damme, K., Nies, A.T., Schaeffeler, E., Schwab, M., 2011. Mammalian MATE (SLC47A) transport proteins: impact on efflux of endogenous substrates and xenobiotics. *Drug Metab. Rev.* 43, 499–523. <https://doi.org/10.3109/03602532.2011.602687>.
- Engel, K., Wang, J., 2005. Interaction of organic cations with a newly identified plasma membrane monoamine transporter. *Mol. Pharmacol.* 68, 1397–1407. <https://doi.org/10.1124/mol.105.016832>.
- Gyntner, M., Pickering, D.S., Spicer, J.A., Denny, W.A., Huttunen, K.M., 2016. Systemic and brain pharmacokinetics of perforin inhibitor prodrugs. *Mol. Pharm.* 13, 2484–2491. <https://doi.org/10.1021/acs.molpharmaceut.6b00217>.
- Higuchi, K., Kitamura, A., Okura, T., Deguchi, Y., 2015. Memantine transport by a proton-coupled organic cation antiporter in hCMEC/D3 cells, an in vitro human blood-brain barrier model. *Drug Metab. Pharmacokinet.* 30, 182–187. <https://doi.org/10.1016/j.dmpk.2014.12.006>.
- Ito, S., Kusuhara, H., Kuroiwa, Y., Wu, C., Moriyama, Y., Inoue, K., Kondo, T., Yuasa, H., Nakayama, H., Horita, S., Sugiyama, Y., 2010. Potent and specific inhibition of mMate1-mediated efflux of type I organic cations in the liver and kidney by pyrimethamine. *J. Pharmacol. Exp. Ther.* 333, 341–350. <https://doi.org/10.1124/jpet.109.163642>.
- Kitamura, A., Higuchi, K., Okura, T., Deguchi, Y., 2014. Transport characteristics of tramadol in the blood-brain barrier. *J. Pharm. Sci.* 103, 3335–3341. <https://doi.org/10.1002/jps.24129>.
- Li, R.W., Yang, C., Sit, A.S., Kwan, Y.W., Lee, S.M., Hoi, M.P., Chan, S.-W., Hausman, M., Vanhoutte, P.M., Leung, G.P., 2014. Uptake and protective effects of ergothioneine in human endothelial cells. *J. Pharmacol. Exp. Ther.* 350, 691–700. <https://doi.org/10.1124/jpet.114.214049>.
- Li, H., Liu, L., Zhu, S., Liu, Q., 2016. Case reports of aconite poisoning in mainland China from 2004 to 2015: a retrospective analysis. *J. Forensic Leg. Med.* 42, 68–73. <https://doi.org/10.1016/j.jflm.2016.05.016>.
- Liu, S., Li, F., Li, Y., Li, W., Xu, J., Du, H., 2017. A review of traditional and current methods used to potentially reduce toxicity of Aconitum roots in Traditional Chinese Medicine. *J. Ethnopharmacol.* 207, 237–250. <https://doi.org/10.1016/j.jep.2017.06.038>.
- Mizuuchi, H., Katsura, T., Ashida, K., Hashimoto, Y., Inui, K., 2000. Diphenhydramine transport by pH-dependent tertiary amine transport system in Caco-2 cells. *Am. J. Physiol. Gastrointest. Liver Physiol.* 278, G563–G569. <https://doi.org/10.1152/ajpgi.2000.278.4.G563>.
- Nyirimigabo, E., Xu, Y., Li, Y., Wang, Y., Agyemang, K., Zhang, Y., 2015. A review on phytochemistry, pharmacology and toxicology studies of Aconitum. *J. Pharm. Pharmacol.* 67, 1–19. <https://doi.org/10.1111/jphp.12310>.
- Ohtsuki, S., Ikeda, C., Uchida, Y., Sakamoto, Y., Miller, F., Glacial, F., Declèves, X., Scherrmann, J.-M., Couraud, P.-O., Kubo, Y., Tachikawa, M., Terasaki, T., 2013. Quantitative targeted absolute proteomic analysis of transporters, receptors and junction proteins for validation of human cerebral microvascular endothelial cell line hCMEC/D3 as a human blood-brain barrier model. *Mol. Pharm.* 10, 289–296. <https://doi.org/10.1021/mp3004308>.
- Okura, T., Hattori, A., Takano, Y., Sato, T., Hammarlund-Udenaes, M., Terasaki, T., Deguchi, Y., 2008. Involvement of the pyrimidine transporter, a putative organic cation transporter, in blood-brain barrier transport of oxycodone. *Drug Metab. Dispos.* 36, 2005–2013. <https://doi.org/10.1124/dmd.108.022087>.
- Okura, T., Kato, S., Deguchi, Y., 2014. Functional expression of organic cation/carnitine transporter 2 (OCTN2/SLC22A5) in human brain capillary endothelial cell line hCMEC/D3, a human blood-brain barrier model. *Drug Metab. Pharmacokinet.* 29, 69–74. <https://doi.org/10.2133/dmpk.DMPK-13-RG-058>.
- Poller, B., Gutmann, H., Krähenbühl, S., Weksler, B., Romero, I., Couraud, P.-O., Tuffin, G., Drewe, J., Huwyler, J., 2008. The human brain endothelial cell line hCMEC/D3 as a human blood-brain barrier model for drug transport studies. *J. Neurochem.* 107, 1358–1368. <https://doi.org/10.1111/j.1471-4159.2008.05730.x>.
- Ren, M.-Y., Yu, Q.-T., Shi, C.-Y., Luo, J.-B., 2017. Anticancer activities of C18-, C19-, C20-, and bis-diterpenoid alkaloids derived from genus Aconitum. *Molecules* 22, 267. <https://doi.org/10.3390/molecules22020267>.
- Sadiq, M.W., Borgs, A., Okura, T., Shimomura, K., Kato, S., Deguchi, Y., Jansson, B., Björkman, S., Terasaki, T., Hammarlund-Udenaes, M., 2011. Diphenhydramine active uptake at the blood-brain barrier and its interaction with oxycodone in vitro and in vivo. *J. Pharm. Sci.* 100, 3912–3923. <https://doi.org/10.1002/jps.22567>.
- Shimomura, K., Okura, T., Kato, S., Couraud, P.-O., Scherrmann, J.-M., Terasaki, T., Deguchi, Y., 2013. Functional expression of a proton-coupled organic cation (H⁺/OC) antiporter in human brain capillary endothelial cell line hCMEC/D3, a human blood-brain barrier model. *Fluids Barriers CNS* 10, 8. <https://doi.org/10.1186/2045-8118-10-8>.
- Singhuber, J., Zhu, M., Prinz, S., Kopp, B., 2009. Aconitum in traditional Chinese medicine: a valuable drug or an unpredictable risk. *J. Ethnopharmacol.* 126, 18–30. <https://doi.org/10.1016/j.jep.2009.07.031>.
- Takahashi, Y., Nishimura, T., Higuchi, K., Noguchi, S., Tega, Y., Kurosawa, T., Deguchi, Y., Tomi, M., 2018. Transport of pregabalin via L-type Amino acid transporter 1 (SLC7A5) in human brain capillary endothelial cell line. *Pharm. Res.* 35, 246. <https://doi.org/10.1007/s11095-018-2532-0>.
- Tega, Y., Akanuma, S., Kubo, Y., Hosoya, K., 2015. Involvement of the H⁺/organic cation antiporter in nicotine transport in rat liver. *Drug Metab. Dispos.* 43, 89–92. <https://doi.org/10.1124/dmd.115.060001>.

- doi.org/10.1124/dmd.114.061002.
- Wang, X., Qi, B., Su, H., Li, J., Sun, X., He, Q., Fu, Y., Zhang, Z., 2017. Pyrilamine-sensitive proton-coupled organic cation (H⁺/OC) antiporter for brain-specific drug delivery. *J. Control. Release* 254, 34–43. <https://doi.org/10.1016/j.jconrel.2017.03.034>.
- Weksler, B., Romero, I.A., Couraud, P.-O., 2013. The hCMEC/D3 cell line as a model of the human blood brain barrier. *Fluids Barriers CNS* 10, 16. <https://doi.org/10.1186/2045-8118-10-16>.
- Wu, C., Sun, X., Feng, C., Liu, X., Wang, H., Feng, F., Zhang, J., 2016. Proton-coupled organic cation antiporter contributes to the hepatic uptake of matrine. *J. Pharm. Sci.* 105, 1301–1306. [https://doi.org/10.1016/S0022-3549\(15\)00190-2](https://doi.org/10.1016/S0022-3549(15)00190-2).
- Wu, J.-J., Guo, Z.-Z., Zhu, Y.-F., Huang, Z.-J., Gong, X., Li, Y.-H., Son, W.-J., Li, X.-Y., Lou, Y.-M., Zhu, L.-J., Lu, L.-L., Liu, Z.-Q., Liu, L., 2018. A systematic review of pharmacokinetic studies on herbal drug Fuzi: implications for Fuzi as personalized medicine. *Phytomedicine* 44, 187–203. <https://doi.org/10.1016/j.phymed.2018.03.001>.
- Yang, C., Zhang, T., Li, Z., Xu, L., Liu, F., Ruan, J., Liu, K., Zhang, Z., 2013. P-glycoprotein is responsible for the poor intestinal absorption and low toxicity of oral aconitine: in vitro, in situ, in vivo and in silico studies. *Toxicol. Appl. Pharmacol.* 273, 561–568. <https://doi.org/10.1016/j.taap.2013.09.030>.
- Ye, L., Yang, X., Yang, Z., Gao, S., Yin, T., Liu, W., Wang, F., Hu, M., Liu, Z., 2013. The role of efflux transporters on the transport of highly toxic aconitine, mesaconitine, hypaconitine, and their hydrolysates, as determined in cultured Caco-2 and transfected MDCKII cells. *Toxicol. Lett.* 216, 86–99. <https://doi.org/10.1016/j.toxlet.2012.11.011>.
- Zhang, Q., Chen, X., Luo, Y., Ren, H., Qiao, T., 2017. Fuzi enhances anti-tumor efficacy of radiotherapy on lung cancer. *J. Cancer* 8, 3945–3951. <https://doi.org/10.7150/jca.22162>.
- Zhou, G., Tang, L., Zhou, X., Wang, T., Kou, Z., Wang, Z., 2015. A review on phytochemistry and pharmacological activities of the processed lateral root of Aconitum carmichaelii Debeaux. *J. Ethnopharmacol.* 160, 173–193. <https://doi.org/10.1016/j.jep.2014.11.043>.
- Zhou, F., Zhu, L., Wang, K., Murray, M., 2017. Recent advance in the pharmacogenomics of human Solute Carrier Transporters (SLCs) in drug disposition. *Adv. Drug Deliv. Rev.* 116, 21–36. <https://doi.org/10.1016/j.addr.2016.06.004>.
- Zhu, L., Wu, J., Zhao, M., Song, W., Qi, X., Wang, Y., Lu, L., Liu, Z., 2017. Mdr1a plays a crucial role in regulating the analgesic effect and toxicity of aconitine by altering its pharmacokinetic characteristics. *Toxicol. Appl. Pharmacol.* 320, 32–39. <https://doi.org/10.1016/j.taap.2017.02.008>.